Environment International 166 (2022) 107395

Contents lists available at ScienceDirect

Environment International

journal homepage: www.elsevier.com/locate/envint

Full length article

Size-based effects of anthropogenic ultrafine particles on activation of human lung macrophages

Simone Marcella [a,1], Barbara Apicella [b,1], Agnese Secondo [c,1], Francesco Palestra [a], Giorgia Opromolla [d], Renato Ciardi [a], Valentina Tedeschi [c], Anne Lise Ferrara [a,e], Carmela Russo [b], Maria Rosaria Galdiero [a,e], Leonardo Cristinziano [a], Luca Modestino [a], Giuseppe Spadaro [a], Alfonso Fiorelli [d], Stefania Loffredo [a,e,*]

[a] Department of Translational Medical Sciences and Center for Basic and Clinical Immunology Research (CISI), University of Naples Federico II, WAO Center of Excellence, 80131 Naples, Italy
[b] Istituto di Scienze e Tecnologie per l'Energia e la Mobilità Sostenibili (STEMS)-CNR, 80125 Naples, Italy
[c] Department of Neuroscience, Reproductive and Odontostomatological Sciences, University of Naples Federico II, 80131 Naples, Italy
[d] Translational Medical and Surgical Science, University of Campania Luigi Vanvitelli, 80131 Naples, Italy
[e] Institute of Experimental Endocrinology and Oncology (IEOS), National Research Council, 80131 Naples, Italy

ARTICLE INFO

Handling Editor: Adrian Covaci

Keywords:
Nanoparticles
Cytokines
Chemokines
Lung
Macrophages
Monocytes
Monocyte-derived macrophages
Calcium homeostasis
ROS
Air pollution
PM

ABSTRACT

The anthropogenic particulate matter (PM), suspended air dust that can be inhaled by humans and deposited in the lungs, is one of the main pollutants in the industrialized cities atmosphere. Recent studies have shown that PM has adverse effects on respiratory diseases. These effects are mainly due to the ultrafine particles (PM0.1, PM $<$ 100 nm), which, thanks to their PM size, are efficiently deposited in nasal, tracheobronchial, and alveolar regions. Pulmonary macrophages are a heterogeneous cell population distributed in different lung compartments, whose role in inflammatory response to injury is of particular relevance. In this study, we investigated the effect of PM0.1 on Human Lung Macrophages (HLMs) activation evaluated as proinflammatory cytokines and chemokine release, Reactive Oxygen Species (ROS) production and intracellular Ca^{2+}concentration ($[Ca^{2+}]_i$). Furthermore, PM0.1, after removal of organic fraction, was fractionated in nanoparticles both smaller (NP20) and bigger (NP100) than 20 nm by a properlydeveloped analytical protocol, allowed isolating their individual contribution. Interestingly, while PM0.1 and NP20 induced stimulatory effects on HLM cytokines release, NP100 had not effect. In particular, PM0.1 induced IL-6, IL-1β, TNF-α, but not CXCL8, release from HLMs. Moreover, PM0.1, NP20 and NP100 did not induce β-glucuronidase release, a preformed mediator contained in HLMs. The long time necessary for cytokines release (18 h) suggested that PM0.1 and NP20 could induce *ex-novo* production of the tested mediators. Accordingly, after 6 h of incubation, PM0.1 and NP20 induced mRNA expression of IL-6, TNF-α and IL-1β. Moreover, NP20 induced ROS production and $[Ca^{2+}]_i$ increase in a time-dependent manner, without producing cytotoxicity.

Collectively, the present data highlight the main proinflammatory role of NP20 among PM fractions. This is particularly of concern because this fraction is not currently covered by legal limits as it is not easily measured at the exhausts by the available technical methodologies, suggesting that it is mandatory to search for new monitoring techniques and strategies for limiting NP20 formation.

Abbreviations: [Ca2+]i, intracellular calcium concentration; ROS, Reactive oxygen species; PM, particulate matter; NP, nanoparticles.

* Corresponding author at: Department of Translational Medical Sciences and Center for Basic and Clinical Immunology Research (CISI), University of Naples Federico II, Via S. Pansini 5, 80131 Naples, Italy.

E-mail addresses: s.marcella92@gmail.com (S. Marcella), barbara.apicella@stems.cnr.it (B. Apicella), secondo@unina.it (A. Secondo), f.palestra97@gmail.com (F. Palestra), gi.opromolla1@gmail.com (G. Opromolla), renato.ciardi@libero.it (R. Ciardi), valentina.tedeschi@unina.it (V. Tedeschi), annelisefarrara@gmail.com (A.L. Ferrara), carmela.russo@stems.cnr.it (C. Russo), mrgaldiero@libero.it (M. Rosaria Galdiero), l.cristinziano@gmail.com (L. Cristinziano), modestinoluca@gmail.com (L. Modestino), spadaro@unina.it (G. Spadaro), alfonso.fiorelli@unicampania.itd (A. Fiorelli), stefania.loffredo2@unina.it (S. Loffredo).

[1] These authors have worked together on a publication and contributed equally.

https://doi.org/10.1016/j.envint.2022.107395
Received 22 March 2022; Received in revised form 31 May 2022; Accepted 4 July 2022
Available online 7 July 2022
0160-4120/© 2022 The Authors. Published by Elsevier Ltd. This is an open access article under the CC BY-NC-ND license (http://creativecommons.org/licenses/by-nc-nd/4.0/).

1. Introduction

Air pollution is one of the leading preventable threats to public health. Atmospheric particulate matter (PM) is recognized as the major air pollutant, and one of the main contributors to the global burden of disease (Butt et al., 2017). The PM of anthropogenic origin is mainly due to motor vehicle emissions and industrial combustion, and cover the fine (PM2.5, PM < 2.5 μm) up to almost all the ultrafine (PM0.1, PM < 0.1 μm) particulate matter fraction (Karagulian et al., 2017). However, the detection in atmosphere of PM0.1, which is inhaled breathing polluted air, is difficult to achieve in the most polluted urban areas as the current technical methodologies are not sensitive toward particles in nanometric size range. In this way, the legal limits of PM0.1 are far from being established. In particular, the main concern about combustion-generated particles arises because of the emissions in the atmosphere of a large number of sub-20 nm particles with negligible mass with respect to the bigger particles (Pedata et al., 2015). These particles (called nanoparticles, NPs) are formed by new technologies combustion systems, where the biggest particles are blocked by abatement systems while the smaller ones are largely emitted into the atmosphere. NPs are not easily measured at the exhausts and in the atmosphere and this feature has prevented overtime an exhaustive study of their biological activity.

It is established that the different PM fractions have a recognized lung and cardiovascular toxicity (Simkhovich et al., 2008; De Falco et al., 2017). In particular, PM concentrations are considered as one of the main factors for adverse health effects (Karagulian et al., 2017; Simkhovich et al., 2008; Pope et al., 2009; Englert, 2004; Brunekreef and Holgate, 2002). PM is suspended air dust that can be inhaled by humans and deposited in the lungs. Recent studies have shown that PM has adverse effects on respiratory diseases because it is deposited in several lung compartment regions (Simkhovich et al., 2008; Kreyling et al., 2006). In the lung tissue, macrophages are the most abundant immune cell type and play a key role in inflammatory and phagocytic processes, tissue damage and repair, angiogenesis and neoplastic growth (Sica and Mantovani, 2012; Granata et al., 2010; Ferrara et al., 2021; Bonavita et al., 2015). Macrophages are a highly heterogeneous cell population distributed in different lung regions (Sica and Mantovani, 2012; Mantovani et al., 2013) . To date, there are no data on the effects of anthropogenic PM and its fractions, such as PM0.1, on human resident macrophages activation as well as on Reactive Oxygen Species (ROS) production and intracellular Ca^{2+} changes. Considering the impact of air pollution on health lung, in this paper we investigated the effect of PM0.1 on proinflammatory cytokine and chemokine release from human lung macrophages (HLMs). In addition, we evaluated ROS production and Ca^{2+} homeostasis, two modulators of inflammatory response as well as of other immunological functions.

Moreover, in order to deep the understanding of the correlation between biologic effect and particle size, the PM0.1 were deprived of organic carbon (OC) with dichloromethane (DCM) extraction. Indeed, it is well known that the chemical composition is essential to determine the cellular responses (Mantecca et al., 2010; Farina et al., 2011) , but since in the present work our goal is not the study of the OC effect, which will be the object of a future work, but of the particle size effect, we studied the particles deprived of OC. Particles were also further separated into two size-segregated fractions, studying separately their effect. The fractions obtained by a properly developed analytical protocol were called: nanoparticles < 20 nm (NP20) and 20 nm < nanoparticles < 100 nm (NP100).

Therefore, even if biological effects of PM0.1 have been already investigated (Longhin et al., 2016), in the present paper the effect of nanometric particulate size has been studied on human lung macrophage functions in the absence of OC.

It was shown that the main toxic effect is presented by NP20, which constitute the fraction more difficult to be monitored and abated from the exhausts. This is an important acquisition from a human health perspective, especially in the context of respiratory disease and its connection with air pollution.

2. Materials and methods

2.1. Ultrafine particulate isolation

Carbon particulate matter was sampled in a lab-scale combustion system consisting of an ethylene-oxygen premixed laminar atmospheric flame (equivalence ratio, $\Phi = 1$, cold gas velocity = 4 cm/s) burning on a water-cooled sintered bronze McKenna burner (d = 60 mm) (Holthuis & Associates, CA, USA). The set-up for the deposition into the flame was constituted of a glass plate horizontally inserted into the flame and rotating by a gear motor with a rotation speed of 1.4gear/s, as shown in the sketch reported in Fig. 1 . The insertion/deposition time of the plate was regulated at 60 ms per lap to avoid plate and sample heating. The total deposition time for each sample was set to 25 s. PM, caught on plates, was first extracted with dichloromethane (DCM) and then filtered, for separating the organic carbon soluble in DCM (OC), from the insoluble ultrafine particles (<100 nm), named PM0.1. PM0.1, collected on the filter, were dispersed in dimethyl sulfoxide (DMSO) and further filtered on 20 nm pore size Anotop filters (Whatman), getting particles <20 nm in DMSO solution (NP20, constituting the 25% in weight of the total PM0.1 sample in the employed experimental conditions) and particles >20 nm and <100 nm (NP100) on the filter, which were again dispersed in DMSO. More details on the flame structure and the sampling and separation set-up are reported in (Russo et al., 2020; Apicella et al., 2002). OC was characterized in detail in several previous works (Apicella et al., 2022 and references therein) and it was found to be constituted of polycyclic aromatic hydrocarbons (PAHs) and high molecular weight aromatic species. By contrast, the PM0.1, insoluble in DCM, were characterized and found to be constituted almost completely by carbon with a low percentage of hydrogen (typically H/C is around 0.1 (Russo et al., 2017 and references therein).

2.2. Reagents

The following reagents were purchased for the experiments: L-glutamine, fetal bovine serum (FBS), detoxified LPS (from *Escherichia coli* serotype 026:B6), Percoll®, piperazine- *N*, *N*_-bis-2-ethanesulphonic acid (PIPES), phosphate buffer saline (PBS), Triton X-100, phenolphthalein β-D-glucuronide sodium salt, Phospholipase IA (from N*aja mossambica mossambica* venom) (svGIA) (Sigma-Aldrich® 155 St. Louis, MO, USA), antibiotic–antimycotic solution (10.000 IU/ml penicillin, 10 mg/ml streptomycin and 25 μg/ml amphotericin B) (Lonza, Basel, CH), RPMI 1640 (Microgem®, Naples, Italy), Histopaque-1077 (GE Healthcare Bio-Sciences AB SE-751 84 Uppsala, Sweden), Target-specific primers for *TNFα*, *IL-6*, *CXCL8, IL-1β* and *GAPDH* were designed using the Beacon Designer 3.0 (BioRad Laboratories, Milan, Italy) and produced and purified by Custom Primers (Life Technologies, Milan, Italy). DMSO (Merck Millipore, Burlington, Massachusetts, USA).

2.3. Isolation and purification of human lung macrophages (HLMs)

Macrophages were purified from macroscopically normal lung tissue of patients (hepatitis C virus−, hepatitis B surface Ag−, HIV1−) undergoing lung resection. The study protocol was approved from the Ethics Committee of University of Naples Federico II (Prot. 7/19), and informed consent was obtained from patients undergoing thoracic surgery. Lung tissue was minced finely with scissors, washed with PIPES buffer over Nitex cloth (120-μm pore size; Sefar Italia) and the dispersed cells recovered. The macrophage suspension was enriched (75–85%) by flotation over discontinuous Percoll density gradients. The cells were suspended (10^6 cells/ml) in RPMI 1640 supplemented with 2 mM L-glutamine, 1% antibiotic–antimycotic solution and 1% non-essential amino acids and incubated in 24-well plates. After 18 h, the medium

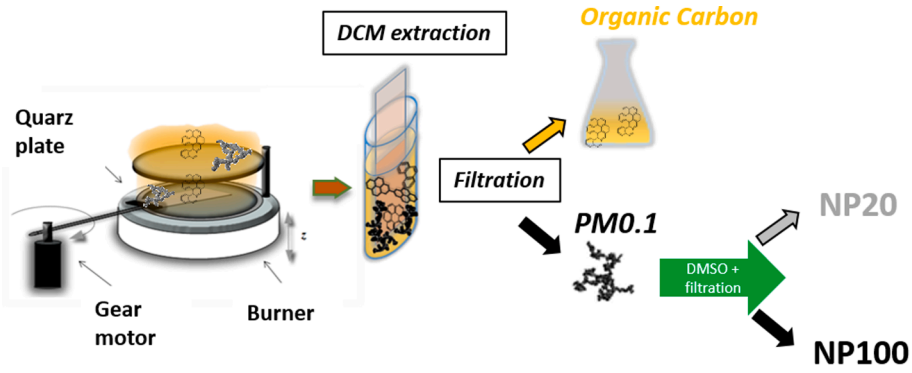

Fig. 1. Sketch of the lab-scale combustion system with the set-up for sampling and separation of particles.

was removed and the plates were gently washed with fresh medium. More than 98% of adherent cells were macrophages, as evaluated by flow-cytometric analysis as previously demonstrated in our publications (Balestrieri et al., 2021).

2.4. Isolation and purification of human monocyte and monocyte-derived macrophages (MDMs)

The study protocol involving the use of human blood cells was approved by the Ethical Committee of the University of Naples Federico II, and written informed consent was obtained from blood donors in accordance with the principles expressed in the Declaration of Helsinki (Protocol number 301/12). Peripheral blood mononuclear cells (PBMCs) were isolated from buffy coats of healthy donors (HBsAg−, HCV−, and HIV−) obtained from a leukapheresis unit. Leukocytes were separated from erythrocytes by dextran sedimentation. PBMCs were purified by Histopaque-1077 density gradient centrifugation (400*g* for 20 min at 22 °C). Monocytes were purified with CD14 microbeads (Miltenyi Biotec, Italy) according to the manufacturer's protocol. To obtain monocyte-derived macrophages (MDMs), monocytes (10^6 cells/cm^2) were differentiated with M-CSF 50 ng/ml (Miltenyi Biotec, Italy) for 7 days in RPMI 1640 supplemented with 10% FBS (Sigma-Aldrich, Italy) (Braile et al., 2021). Finally the cells were used for experiments.

2.5. Cell cultures and treatments

HLMs, monocytes and MDMs were incubated (37 °C, 5% CO_2, 18 h) in RPMI 1640 supplemented with 5% FBS, 2 mM/l L-glutamine, 1% antibiotic–antimycotic solution and 1% non-essential amino acid. After 24 h, cells were stimulated with increasing concentrations of UPFs (0.25–4 ppm), NP20 (0.15–2.5 ppm) or NP100 (0.25–4 ppm) for 6 and 18 h. These time points have been chosen in consideration of previous studies. Concentrations of particles are expressed in ppm i.e. part per millions of particles in the DMSO solvent (micrograms/grams). LPS was added as internal positive control at the maximal concentration (1 μg/ml for HLMs and 100 ng/ml for monocytes and MDMs) for 18 h. At the end of incubation, supernatants were harvested, centrifuged (300*g*, 4 °C, 5 min) and stored at −80 °C for the subsequent determination of TNF-α, IL-6, CXCL8, IL-1β and β-Glucuronidase release. Lysis of the cells remaining in the plates was carried out by using 0.1% Triton X-100 for total protein quantification by a Bradford assay (BioRad).

2.6. Cell viability

After treatments, cell viability was evaluated as mitochondrial activity, determined by the MTT (3-(4,5-dimethylthiazol-2-yl)2,5-diphenyl tetrazolium bromide) assay, as reported previously (Scorziello et al., 2004), in which a proper description of cell viability test has been done. HLMs, monocytes and MDMs were incubated with PM0.1, NP20 and NP100, 1% v/v Triton X-100 or medium alone for the time indicated. At the end of the incubation, supernatants were removed and the cells were incubated (37 °C, 1 hr) in 1 mL of MTT solution (0.5 mg/mL). Cells were washed with PBS, 0.5 mL of DMSO was added, and absorbance was read at 540 nm. Cell injury is expressed as a percentage of cultures treated with medium alone.

2.7. ELISA assays

The release of soluble mediators in the supernatants of HLMs, monocytes and MDMs was measured in duplicate using commercially available ELISA kits for TNFα, IL-6, CXCL8 (R&D Systems, Minneapolis, MN) and IL-1β (Thermo Fisher Scientific Wilmington, DE, USA). Since the number of HLMs, monocytes and MDMs can vary among the wells and different experiments, the results obtained were normalized for the total protein content in each well, determined in the cell lysates (0.1% Triton X-100) by the Bradford assay. Therefore all cytokines values were expressed as ng/mg of total proteins.

2.8. β-Glucuronidase release

β-Glucuronidase release was measured in cell-free supernatants or in cell lysates by a colorimetric assay. Supernatants and cell lysates were incubated (37° C, 18 h) with 0.1 M acetate buffer (pH 4.5) containing phenolphthalein β-D-glucuronide. At the end of incubation glycine buffer was added to each tube and the mixture was subjected to optical density (OD) reading at 540 nm. β-Glucuronidase release was expressed as the percentage of the total cellular content determined in cells lysed with 0.1% Triton X-100. All experiments were performed in duplicate determinations.

2.9. RT-PCR

TNF-α, IL-6, CXCL8 and IL-1β mRNA expression was also investigated. Cells (1.5×10^5 /per well) were incubated (37 C, 5% CO_2, 6 h) with LPS (1 μg/ml for HLMs and 100 ng/ml for monocytes and MDMs), PM0.1 (4 ppm), NP20 (2.5 ppm) or NP100 (4 ppm) alone respectively. After stimulation supernatants were removed, whereas cells were lysed, to evaluate *TNF-α, IL-6, CXCL8* and *IL-1β mRNA* expression. Total RNA was extracted by TRIzol reagent (Euroclone®, Pero, Milan, Italy) following the manufacturer's instructions. RNA quality and integrity were estimated by spectrophotometric analysis on a Nanodrop ND-1000 spectrophotometer (Thermo Fisher Scientific, Wilmington, DE, USA) and by 1% (w/v) agarose gel electrophoresis (see Supplementary Fig. 1). Reverse transcription was performed using the High-Capacity cDNA Reverse Transcription Kit (Applied Biosystems, Foster City CA, USA). Real-time RT-PCR was performed by means of Universal SYBR Green Supermix (Bio-Rad) on a CFX96 Real-time detection system (Bio-Rad). GAPDH was used as housekeeping gene to normalize Ct (cycle threshold) values using the $2^{-\Delta Ct}$ formula. PCR efficiency and specificity were evaluated by analyzing amplification curves with serial dilutions of

the template cDNA and their dissociation curves. Each cDNA sample was analyzed in triplicate and the sample without reverse transcriptase was included as a negative control. The data were analyzed with iCycleriQ analysis software (Bio-Rad) and the changes in *TNFα, IL-6, CXCL8* and *IL-1β mRNAs* were expressed as $2^{-\Delta Ct}$.

2.10. Reactive oxygen species (ROS) production

HLMs were incubated for 30 min after the addition of 10 μg/ml 2′,7′-dichlorodihydrofluorescein diacetate (H_2DCF-DA) (Life Technologies, Milan, Italy). H_2DCF-DA is a fluorogenic dye that allows the evaluation of hydroxyl, peroxyl and other ROS activities within the cell. Once diffused into the cell, H_2DCF is deacetylated by cellular esterases to a nonfluorescent molecule, which is oxidized by ROS into 2′,7′-DCF. This latter compound is highly fluorescent and can be determined by fluorescence spectroscopy with maximum excitation and emission wavelengths of 492–495 nm and 517–527 nm, respectively. Cells were washed in PBS, then resuspended in RPMI supplemented with 5% of FBS and finally seeded in a 96-well precoated plate with medium alone, NP20 (2.5 ppm) or PM0.1 (4 ppm). Finally, immediately after stimulation, the plate was placed in an EnSpire Multimode Plate Reader (Perkin Elmer). The ability of stimuli to induce cytoplasmic ROS-catalyzed oxidation of H_2DCF in HLMs was measured as compared to the negative control (the medium alone). The data were expressed as 2′,7′-DCF mean fluorescence intensity (MFI) measured up to 20 min with 10 min span at an excitation wavelength of 492–495 nm and emission at 517–527 nm.

2.11. $[Ca^{2+}]_i$ measurement on single-cell

HLMs cultured on poly-L-lysine–coated glass coverslips were loaded with 10 μM Fura-2 AM for 1 h at 37 °C in Krebs-Ringer saline solution (containing the following: 5.5 mM KCl, 160 mM NaCl, 1.2 mM $MgCl_2$, 1.5 mM $CaCl_2$, 10 mM glucose, and 10 mM HEPES-NaOH (pH 7.4)). At the end of the loading period, $[Ca^{2+}]_i$ was monitored by single-cell computer-assisted video imaging (Staiano et al., 2013) with a digital imaging system composed of Zeiss Axiovert 200 microscope (Carl Zeiss, Jena, Germany) equipped with a FLUAR × 40 oil objective lens, MicroMax 512BFT cooled charge-coupled device camera (Princeton Instruments, Trenton, NJ, USA), LAMBDA 10-2 filter wheeler (Sutter Instruments, Novato, CA, USA), and MetaMorph/MetaFluor Imaging System software (Universal Imaging, West Chester, PA, USA). The coverslip containing cells was placed on a perfusion chamber (Medical Systems, Greenvale, NY, USA) and illuminated alternately at 340 and 380 nm by a Xenon lamp. The emitted light was passed through a 512-nm barrier filter. Fura-2 AM fluorescence intensity was measured every 3 s. A total of 25–30 individual cells were selected and monitored simultaneously from each coverslip. The results are presented as the cytosolic $[Ca^{2+}]$. Calibrations used the equation of Grynkiewicz et al., assuming that the K_D for Fura-2 AM was 224 nM (Grynkiewicz et al., 1985). $[Ca^{2+}]_i$ was measured in HLMs incubated with UPFs (4 ppm), NP20 (2.5 ppm) or NP100 (4 ppm) for different time-points (10 min, 20 min and 18 h).

2.12. Macrophage extracellular traps (METs) detection using fluorescence microscopy

HLMs (8×10^5 cells per well) were seeded on 12 mm glass coverslips, previously added into 24 well-plates, and incubated (37 °C, 5% CO_2, 1hr) in RPMI 1640 supplemented with 5% FBS, 2 mM/l L-glutamine, 1% antibiotic–antimycotic solution and 1 %non-essential amino acid to ensure cells adhesion. At the end of incubation cells were stimulated (37 °C, 5% CO_2, 3 h) with medium alone as negative control (CTR), phorbol 12-myristate 13-acetate (PMA,10 ng/ml) as positive control, PM0.1 (4 ppm) and NP20 (2.5 ppm), NP100 (4 ppm). For mitochondrial DNA detection cells were treated and incubated (37 °C, 5% CO_2, 30 min) with 5 μM MitoSOX red (Thermo Fisher Scientific, Waltham, Massachusetts, USA) following the manufacturer's instructions. After removing medium cells were treated (25°C, 10 min) with 5 mM SYTOX green (Thermo Fisher Scientific, Waltham, Massachusetts, USA). After incubation cells were fixed with 4% paraformaldehyde (PFA) for 10 min at room temperature and mounted in a drop of fluorescent mounting medium with 4′,6-Diamidino-2-Phenylindole, Dihydrochloride (DAPI) for DNA staining (Thermo Fisher Scientific, Waltham, Massachusetts, USA). Images of three randomly selected and noncontiguous fields were captured for each coverslip using fluorescence microscopy to accurately represent the effect exerted by the stimuli. Axio Observer 7 with Apo-Tome 2.0 (Carl Zeiss MicroImaging, Jena, Germany), which allows creation of optical sections free of scattered light, was used for fluorescence microscopy. Images were digitized at 63x objective magnification.

2.13. Statistical analysis

The data are expressed as mean values ± SD of the indicated number of experiments. Statistical analysis was performed in Prism 6 (GraphPad Software). Statistical analysis was performed by Student'sttest or one-way analysis of variance followed by Dunnett's test (when comparison was made against a control) or Bonferroni's test (when comparison was made between each pair of groups) by means of Analyse-it for Microsoft Excel, version 2.16 (Analyse-it Software, Ltd., Leeds, United Kingdom). A *p*value $\leq$ 0.05 was considered statistically significant.

3. Results

3.1. Effects of PM0.1, NP20 and NP100 on the release of cytokines and chemokines from HLMs

Upon cellular activation, HLMs express and release several cytokines and chemokines and growth factors such as IL-6, TNF-α, IL-1β and CXCL8 (Ferrara et al., 2021; Balestrieri et al., 2021; Braile et al., 2021). In a series of eight different experiments, we evaluated the effects of PM0.1 and their fraction NP20 and NP100 on HLM activation.

Time-course experiments showed that PM0.1 and NP20, but not NP100, induced, after 18 h of incubation, the release of IL-6 (Fig. 2 A-C) and TNF-α (Fig. 2 D-F) in a concentration-dependent manner. The production of IL-1β was significant induced only by NP20 (Fig. 2 H) because IL-1β release induced by PM0.1 and NP100 was concentration dependent but not significant (Fig. 2 G, H). By contrast, PM0.1 and their fractions had no effect on CXCL-8 release (Fig. 2 L-N). Interestingly, under the same condition, the release of the tested mediators was significant higher upon the stimulation with NP20 compared to PM0.1. LPS, the most abundant component within the cell wall of Gram-negative bacteria, was a potent stimulus for the release of all tested mediators (Fig. 2 A-N).

The percentage of viable HLMs measured by MTT assay 18 h after PM0.1, NP20 and NP100 treatment did not differ from that of untreated cells (data not shown). Analyzing live HLMs, by microscope of high content analysis image system Operetta, after stimulation with PM0.1, NP20 and NP100 we noticed that the morphology and area of treated HLMs were not different to that of untreated cells (Supplementary Fig. 2).

Next experiments were performed to determine whether PM0.1, NP20 and NP100 could induce the release of the lysosomal enzyme β-glucuronidase stored in HLMs. In this set of experiments, cells were incubated (37 °C, 2 h) with different concentrations of PM0.1, NP20 and NP100. Supplementary Fig. 3 shows that NP20 induced, in concentration dependent way, a slight but not significant increase of β-glucuronidase (panel B) by constrast PM0.1 (panel A), and NP100 (panel C) had no effect. Snake venom phospholipase 1A (svGIA) was used as positive control (panel A-C) (Triggiani et al., 2009). These data suggest that there is not degranulation of performed β-glucuronidase induce by

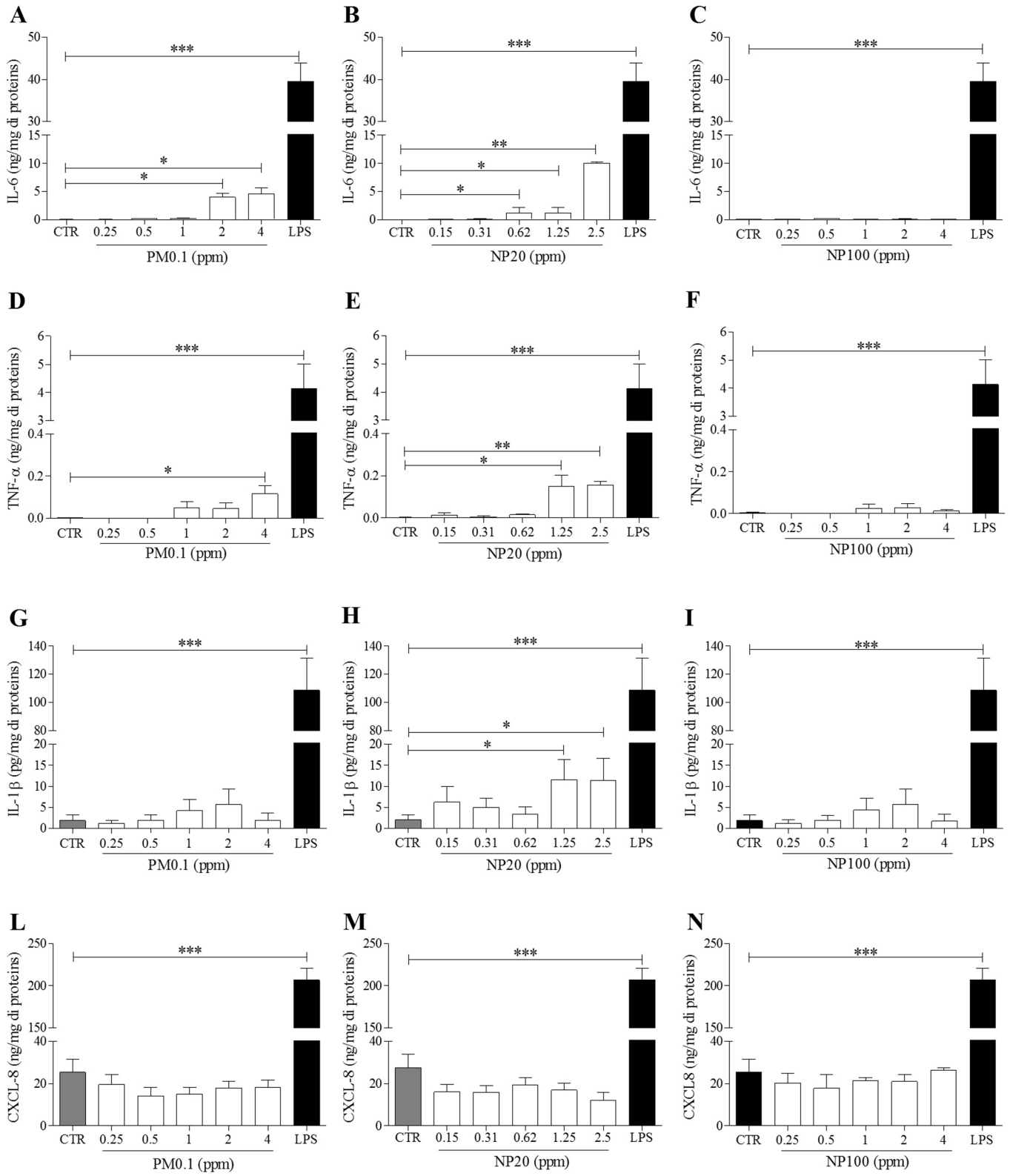

Fig. 2. Effects of PM0.1, NP20 and NP100 on cytokines and chemokines production from HLMs. Highly purified HLMs (1×10^6 cells/well) were stimulated (18 h, 37 °C) with RPMI alone (CTR) or increasing concentrations of PM0.1 (A, D, G, L), NP20 (B, E, H, M), NP100 (C, F, I, N) and LPS (1 μg/ml). IL-6 (A-C), TNF-α (D-F), IL-1β (G-I) and CXCL8 (L-N) proteins in supernatants were evaluated by ELISA. Data are mean ± SD of 8 independent experiments obtained from different patients. * $p < 0.05$, ** $p < 0.01$ and *** $p < 0.001$*vs.*CTR.

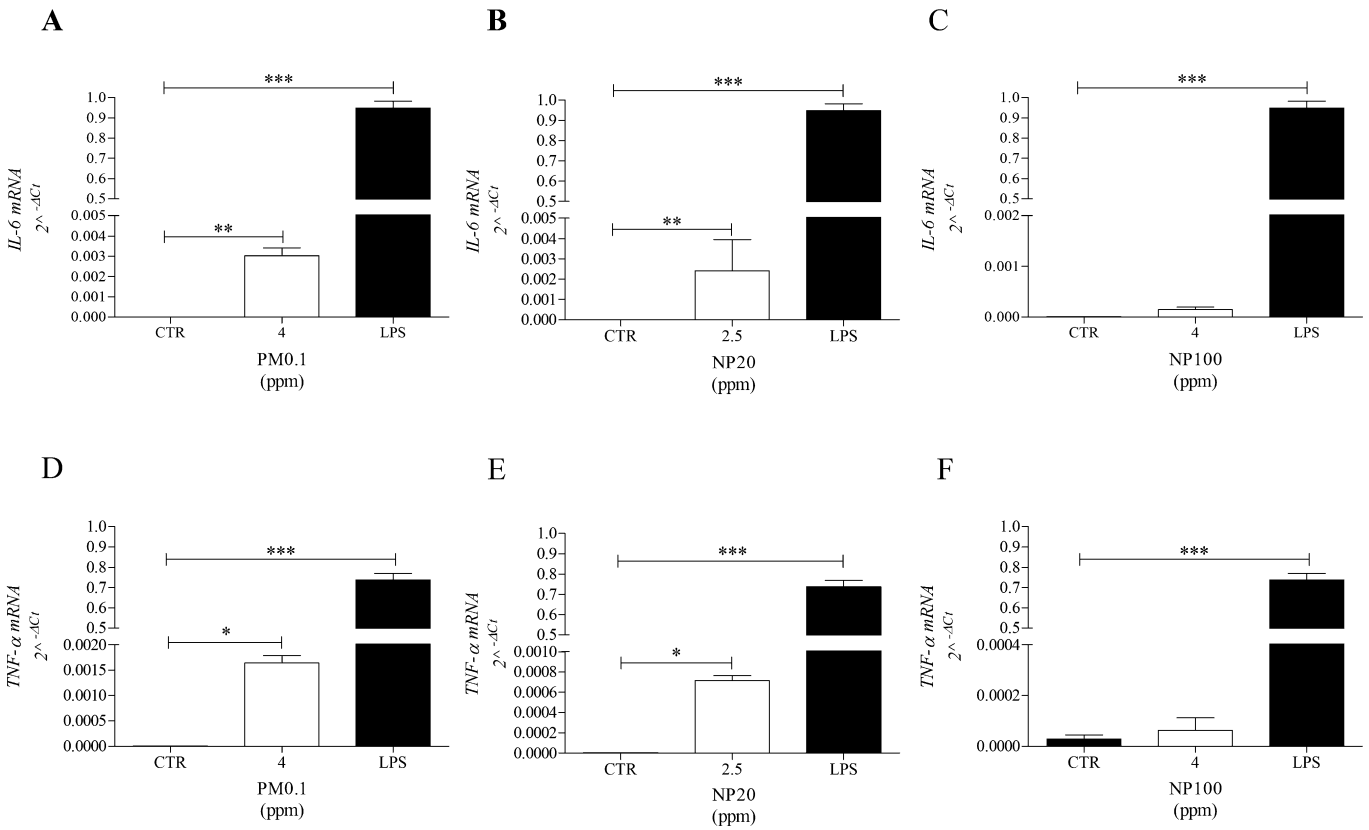

Fig. 3. Effects of PM0.1, NP20 and NP100 on mRNA expression for IL-6 and TNF-α in HLMs. Highly purified HLMs (4.5×10^6 cells/well) were incubated (6 h, 37 °C) in the absence (CTR) or in the presence of PM0.1 (4 ppm), NP20 (2.5 ppm), NP100 (4 ppm) or LPS (1 μg/ml). At the end of incubation, IL-6 (A-C) and TNF-α (D-F) mRNAs were determined by quantitative RT-PCR. Data are mean ± SD of 6 independent experiments obtained from different patients. $^*p < 0.05$, $^{**}p < 0.01$ and $^{***}p < 0.001$ vs. CTR.

any tested stimuli.

Although the use of highly purified PM0.1 in these experiments may exclude the promiscuous effect of LPS contamination, HLMs were stimulated with PM0.1and NP20 in the presence of polymyxin B (50 mg/ml), a potent inactivator of LPS (Bas et al., 2008). Polymyxin B did not influence the capacity of PM0.1 and NP20 to induce IL-6, TNF-α and IL-1β release, whereas it almost completely suppressed the production of cytokines and chemokines induced by LPS (Supplementary Fig. 4).

In the next series of experiments we evaluated if PM0.1, NP20, NP100 activated the mRNA expression for cytokines and chemokines in HLMs by real-time PCR. To perform these experiments we have chosen the tested maximum concentration for PM0.1 (4 ppm), NP20 (2.5 ppm) and NP100 (4 ppm) Both PM0.1 and, but not NP100 (Fig. 3 C-F), markedly increased the proinflammatory *IL-6* (Fig. 3 A-B) and *TNF-α* (Fig. 3 D-E) *mRNA*. LPS was used as positive control (Fig. 3 A-F). Interestingly, after 6 h of stimulation, none of tested particles induced the production of IL-6 and TNF-α (Supplementary Fig. 5). These data indicate that PM0.1 and NP20 induced a proinflammatory profile by cytokine/chemokine production and gene expression from human macrophages.

3.2. Effects of PM0.1, NP20 and NP100 on ROS production and Ca^{2+} homeostasis

Reactive oxygen species (ROS) play an essential role in macrophage activation and polarization (Canton et al., 2021; Staiano et al., 2016). Thus, we evaluated whether PM0.1, NP20 and NP100 could activate ROS production in HLMs. ROS production was induced by NP20 already after 1 min of incubation and reached a peak at 20 min (Fig. 4 A). Conversely PM0.1 and NP100 (Fig. 4A) had no effect on ROS production. Since ROS level strictly depends on the increase in $[Ca^{2+}]_I$ and *vice versa,* we monitored $[Ca^{2+}]_i$ in control HLMs and in HLMs exposed to PM0.1, NP20 and NP100. Time-course experiments revealed that PM0.1 induced a slow but significant increase in $[Ca^{2+}]_i$ after 18 h of exposure while it was ineffective after 10 and 20 min of incubation (Fig. 4 B-C). In contrast, NP20 increased $[Ca^{2+}]_i$ already after 20 min of exposure, unrevealing a more rapid effect on Ca^{2+} signaling (Fig. 4 B-C). This is possibly linked to the higher membrane permeability of NP20 due to their smaller size. Furthermore, in the presence of NP100 for 20 min, $[Ca^{2+}]_i$ did not change in comparison to control level (in control cells $[Ca^{2+}]_i = 42 \pm 8$; in NP100-treated cells $[Ca^{2+}]_i = 44 \pm 5.7$) (Fig. 4C).

3.3. Effect of PM0.1 and their fractions on Macrophage extracellular trap (METs) formation

Several studies have shown that macrophages are capable of producing extracellular traps (ETs) (Doster et al., 2018). To evaluate the release of oxidized mitochondrial DNA from HLMs under PM0.1 and their fractions priming, the cells were incubated (1 hr) with MitoSOX Red and SYTOX green, fixed and mounted with DAPI, and then visualized using an inverted fluorescence microscope. Supplementary Fig. 6 demonstrates that PM0.1 (panel B), NP20 (panel C) and NP100 (panel D) did not induce METs from HLMs, similarly to the cells from the control group (CTR, panel A). Conversely PMA, used as positive control, induced extracellular DNA release (panel E) (Doster et al., 2018).

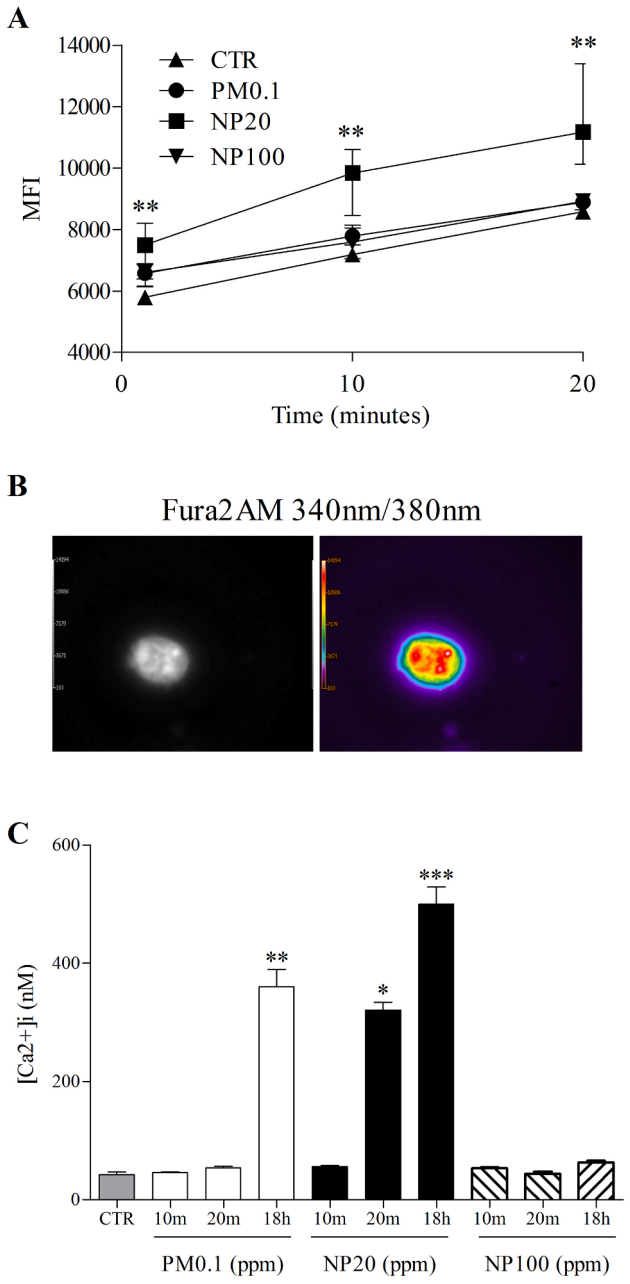

Fig. 4. Effects of PM0.1, NP20 and NP100 on ROS production and $[Ca^{2+}]_i$ in HLMs. (A) 2′,7′-dichlorodihydrofluorescein diacetate-labeled HLMs were stimulated with PM0.1 (4 ppm), NP20 (2.5 ppm) or NP100 (4 ppm), and fluorescence was measured for 20 min at 10-min intervals. Data are mean ± SD of 4 independent experiments with cells from different donors. **p < 0.01 vs CTR. (B) Representative fluorescence image of a single HLM loaded with Fura-2 AM and acquired by video-imaging system. (C)Bar graph depicting the effect of fast and long exposure (10 min, 20 min, 18 h) to PM0.1 (4 ppm), NP20 (2.5 ppm) and NP100 (4 ppm). The experiments have been repeated three times on at least n = 20 cells for each experiment. **p < 0.05 vs CTR, 10 and 20 min PM0.1; *p < 0.05 vs CTR and 10 min NP20; ***p < 0.05 vs CTR, 10 min and 20 min NP20.

3.4. PM0.1 and NP20 effect on monocytes and monocyte-derived macrophages (MDMs)

We also assessed the effect of optimal concentrations of PM0.1 and their fractions in another model of human macrophages such as monocyte-derived macrophages (MDMs) and on their precursors, the peripheral blood monocytes. PM0.1 and NP20 had no effect on IL-6 (Fig. 5 A), TNF-α (Fig. 5 B) and CXCL8 (Fig. 5 C) from freshly isolated monocytes.

Conversely to HLMs, both PM0.1 and NP20 did not induce the release of any tested cytokines, such as IL-6 (Fig. 5 D), TNF-α (Fig. 5 E), IL-1β (Fig. 5 F) and CXCL8 (Fig. 5 G) from MDMs suggesting that activator effects are specific for lung resident macrophages.

4. Discussion

In the present study, we investigated the effect of PM0.1, contained in PM, and their different fractions (i.e. NP20 and NP100) on the release of pro-inflammatory mediators from HLMs. The particles fractions have been deprived of OC by solvent extraction and therefore the main difference is their size. HLMs were isolated from non-tumor human lung tissue from a total of 20 patients who underwent surgery for lung cancer. We demonstrated that NP20, but not NP100, activated HLMs producing IL-6, TNF-α and IL-1β by the induction of gene transcription. Moreover, NP20 induced ROS production and intracellular Ca^{2+}concentration ($[Ca^{2+}]_i$) increase in a time-dependent manner.

Air pollution is a mixture of solid particles and gases in the air. Car emissions, chemicals from factories, dust, pollen and mold spores may be suspended as particles. Several *in vivo* and *in vitro* experiments showed that ambient PM may result in pulmonary inflammation, airway hyper reactivity, alveolar macrophage impairment and epithelial cell damage (Geiser and Kreyling, 2010; Oberdörster et al., 2005). The mechanisms, the efficiency and the regions of particle deposition in the respiratory tract depend on the aerodynamic diameter of the inhaled particles. In particular, PM0.1, the fraction at lower aerodynamic size (<100 nm), deposit with high efficiency in the entire respiratory tract, from the head airways to the alveoli, due to diffusion (Geiser and Kreyling, 2010; Oberdörster et al., 2005). However very few articles have addressed the biological effect of PM0.1 (Longhin et al., 2016) and, as far as we know, it is the first time that the effect of only size (without the contribution of OC) of nanometric fractions of PM0.1 is investigated. The fractions, obtained from PM0.1 by setting a proper analytical protocol (described in the experimental section) and named NP20 and NP100 are <20 nm and <100 nm, respectively, and differ between them mainly for the size. In human lung, resident macrophages, the predominant immune cells, play an important role in orchestrating the initiation and resolution phases of both innate and adaptive immunity (Mantovani et al., 2013). Here we demonstrated that PM0.1were able to activate HLMs in inducing the production of IL-6 and TNF-α. These proinflammatory cytokines are responsible for immune response activation and are secreted by several cells, including macrophages, in response to cell damage caused by infection inflammation or malignant transformation (Tseng et al., 2005; Arango Duque and Descoteaux, 2014). Interestingly, NP20, the smallest component of PM0.1 in terms of both size (<20 nm) and concentration (25% of PM0.1), induced the production of IL-6, TNF-α and IL-1β from HLMs; by contrast NP100 (>20 nm; 75% of PM0.1) had no effect on HLM activation. At the same concentration the effect of NP20 was stronger than that of PM0.1. It is conceivable that the ability of PM0.1to activate HLMs was due only to the presence, even if low, of NP20. We assume that the percentage of NP20 in PM0.1sample was not high enough to detect IL-1β release. Furthermore, PM0.1 and NP20 did not induce release of the HLM preformed mediator β-glucuronidase and CXCL-8. Of note, the results showing that particles NP20 were able to significantly induce IL-6, TNF-α and IL-1β release in respect of their size is a very important aspect, not only for the effect correlated to the entity of the release but also for the downstream pathways that eventually can be modulated.

Macrophages activation could induce the release of preformed and/or *de novo* synthesized mediators. Of note, the effect on IL-6, TNF-α and IL-1β release occurred after 18 h of incubation with PM0.1and NP20, while mRNA expression of IL-6, TNF-α and IL-1β was detected after only 6 h, showing a significant *de-novo* production of the tested mediators. This latter result reflects the ability of PM fractions to induce a local perpetuating inflammation after long-term exposure.

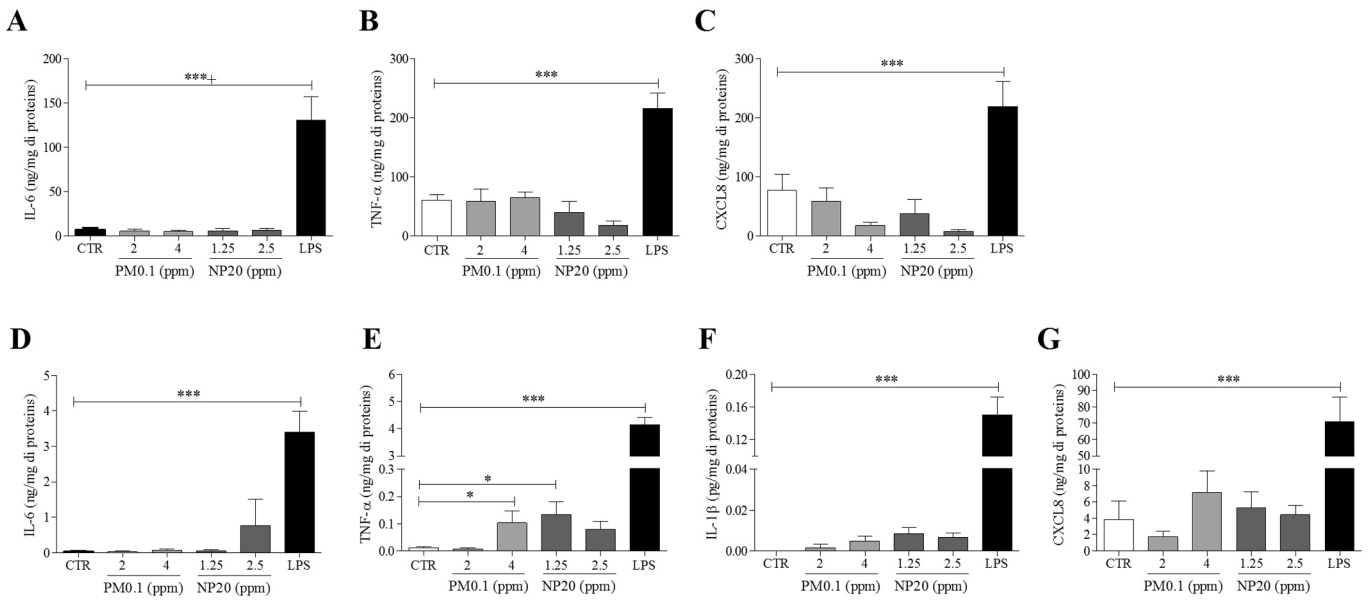

Fig. 5. Effects of PM0.1and NP20 on cytokine and chemokine production by monocytes and MDMs. Monocytes (1×10^6 cells/well)(A-C) and MDMs (1×10^6 cells/well) (D-G) were incubated (18 h, 37 °C) in the presence of PM0.1 (2–4 ppm), NP20 (1.25–2.5 ppm), or LPS (100 ng/ml). At the end of incubations cytokine concentrations in supernatants were evaluated by ELISA. Data are mean ± SD of 6 independent experiments obtained from different healthy donors. * $p < 0.05$, ** $p < 0.01$ and *** $p < 0.001$ vs. CTR.

Another interesting result is that NP20 induced ROS hyperproduction and intracellular Ca^{2+} concentration ($[Ca^{2+}]_i$) increase without producing HLM cytotoxicity. Interestingly, both these intracellular elements (i.e. ROS and Ca^{2+}) may be useful to boost not only the release of cytokines but also their genes' transcription through the modulation of several ionic mechanisms. In particular, Ca^{2+} ions may control distinct functions in dependence of the amplitude and the frequency of own signals, and also in consideration of the channel and/or pump mediating its increase. Our results showed that NP20 induced an initial $[Ca^{2+}]_i$ increase followed by a secondary elevation of its concentration. This may occur through different mechanisms and may control downstream cell immune functions. For example, it has been shown that, airborne PM2.5, having an aerodynamic size larger than that of our nanoparticles, inhibits the activity of the Na^+K^+-ATPase (Geng et al., 2006) thus suggesting a modulatory effect on ionic homeostasis and cell survival. However, $[Ca^{2+}]_i$ increase may be a secondary event triggered by cytokine release. In this respect, $[Ca^{2+}]_i$ increase may occur in two different steps in response to TNF-α release. In lung microvessels, the initial increase corresponds with TNF-α receptor activation. This initial $[Ca^{2+}]_i$ spike may be followed by prolonged elevation of Ca^{2+} that persists even when TNF-α release finished and it is mediated by plasmalemmal receptors and channels (Rowlands et al., 2011).

Although the significant alteration of intracellular ionic homeostasis in HLMs, PM0.1 and NP20 did not produce cytotoxicity in the frame of observation. This is in agreement with previous studies in which PM2.5 exposure did not affect cell viability of rat alveolar macrophages but decreased the amount of mitochondria labelled with Mito-Tracker (Geng et al., 2006). This does not influence the fate of macrophages but possibly determines their M1 polarization by ROS pathway, as observed for PM2.5 exposure (Zhao et al., 2016). On the other hand, higher level of [Ca2+]i could be crucially involved in phagocytic defense, locomotion, migration and intracellular transport.

Furthermore, in support of the present results, it has been shown that a well known chelator of Ca^{2+}, BAPTA-AM, did not suppress cytoskeletal dysfunction induced by ultrafine particles in a clonal macrophage cell line, thus suggesting that the level of this ion per se' does not represent the unique factor inducing macrophage dysfunctions (Moller et al., 2005).

Recent studies have demonstrated that macrophages produce extracellular traps (ETs). METs are produced in response to various stimuli which serve to immobilize and kill microorganisms, but they are also implicated in disease pathology including inflammation and autoimmune disease (Doster et al., 2018). Here we showed that PM0.1 and NP20 had no effect on MET formation unlike PMA used as positive control.

Tissue macrophages are derived from circulating blood monocytes that originate in the bone marrow (Zhao et al., 2018). MDMs are derived from monocytes differentiated to macrophages in the presence of G-CSF (Staiano et al., 2016). In previous publications we reported some biological and immunological differences between primary HLMs and MDMs (Braile et al., 2021; Staiano et al., 2016). It was interesting to observe that both PM0.1 and NP20 did not induce cytokines production from monocytes and MDMs. The differences between the data obtained with HLMs and MDMs could be explained by the different ontogeny of in vitro-derived macrophages (i.e., MDMs) and primary tissue-resident macrophages (i.e., HLMs). Further studies on other tissue macrophages are needed to understand whether the activating effect ofNP20 is specific for macrophages purified from lung. The lung is the most but not only organ affected by pollution, in fact crossing lung blood-air barrier, PM fractions gain access to peripheral circulation reaching the brain via the lung-brain axis (Mühlfeld et al., 2008).

Another important issue is that epidemiological studies show a synergistic effect between PMs and RNA virus infections. It is believed that PMs can facilitate the spread of influenza viruses by providing condensation nuclei for the virus thus being a critical factor for their long-range dissemination and transmission (Weuve et al., 2012). Exposure to diesel engine exhaust, an important source of PMs, from PM10 up to NP20 (Apicella et al., 2020) can generate oxidative stress in human nasal and bronchial epithelial cells and also facilitate the engraftment of the influenza virus to these cells (Zanobetti et al., 2011). Furthermore, epidemiological evidence on the severe acute respiratory syndrome (SARS) outbreak the human coronavirus disease most closely related to Covid-19, revealed that prolonged exposure to air pollution determinants may have a detrimental effect on the prognosis of patients infected with Covid-19 (Woodby et al., 2021; Copat et al., 2020). Lung inflammatory response causes by Covid-19 induces high levels of inflammatory markers, including C-reactive protein, ferritin, D-dimer, and cytokines such as IL-6 and TNF-α in patients with severe diseases (Wang

et al., 2007; Del Valle et al., 2020). Here we demonstrated that the same cytokines were released from PM0.1-activated HLMs. It would be interesting to study the effect of SARS-CoV2 on the production of IL-6 and TNF-α in HLMs and to evaluate whether SARS-CoV2 has a synergistic effect on HLMs activated by PM0.1.

In conclusion NP20 exposure enhances the release and the expression of proinflammatory cytokines and ROS production through $[Ca^{2+}]_i$ changes. This suggests that pulmonary inflammation and oxidative stress conditions induced by air pollutants could be also due to the activation of lung macrophages. Collectively, the present data highlight the main proinflammatory role of NP20 among PM fractions. This is particularly of concern because, although mass emissions of combustion-generated PM have been substantially reduced by new combustion technology, there is still considerable emission into the atmosphere of large numbers of sub-20 nm particles with insignificant mass.

However, this PM fraction is not currently covered by legal limits as it is not easily measured at the exhausts by the available technical methodologies, suggesting that it is necessary to search for new monitoring techniques and strategies limiting NP20 formation and/or release.

Data availability statement

Data supporting the reported results are available upon request.

Institutional review board statement

The study was conducted according to the guidelines of the Declaration of Helsinki, and approved by the Ethics Committee of University of Naples Federico II (Prot. 7/19 and 301/12).

Funding

This work was partially supported an investigator-initiated research grant (grant number:IIT-ITA-002138), MIUR PRIN 2017 M8Y MR8_005. CINECA Awards N. HP10B3JT25 2020, FISM 2018 R4 for the availability of high performance computing resources and support.

Declaration of Competing Interest

The authors declare that they have no known competing financial interests or personal relationships that could have appeared to influence the work reported in this paper.

Appendix A. Supplementary material

Supplementary data to this article can be found online at https://doi.org/10.1016/j.envint.2022.107395.

References

Butt, E.W., Turnock, S.T., Rigby, R., Reddington, C.L., Yoshioka, M., Johnson, J.S., Regayre, L.A., Pringle, K.J., Mann, G.W., Spracklen, D.V., 2017. Global and regional trends in particulate air pollution and attributable health burden over the past 50 years. Environ. Res. Lett. 12 (10), 104017.

Karagulian, F., Van Dingenen, R., Belis, C.A., Janssens-Maenhout, G., Crippa, M., Guizzardi, D., et al., 2017. Attribution of anthropogenic PM2.5 to emission sources A global analysis of source-receptor model results and measured source-apportionment data. JRC. Tech. Rep.

Pedata, P., Stoeger, T., Zimmermann, R., Peters, A., Oberdörster, G., D'Anna, A., 2015. Are we forgetting the smallest, sub 10 nm combustion generated particles? Part. Fibre. Toxicol. 12, 1–4.

Simkhovich, B.Z., Kleinman, M.T., Kloner, R.A., 2008. Air pollution and cardiovascular injury epidemiology, toxicology, and mechanisms. J. Am. Coll. Cardiol. 52 (9), 719–726.

De Falco, G., Colarusso, C., Terlizzi, M., Popolo, A., Pecoraro, M., Commodo, M., Minutolo, P., Sirignano, M., D'Anna, A., Aquino, R.P., Pinto, A., Molino, A., Sorrentino, R., 2017. Chronic Obstructive Pulmonary Disease-Derived Circulating Cells Release IL-18 and IL-33 under Ultrafine Particulate Matter Exposure in a Caspase-1/8-Independent Manner. Front. Immunol. 8.

Pope, C.A., Ezzati, M., Dockery, D.W., 2009. Fine-particulate air pollution and life expectancy in the United States. N. Engl. J. Med. 360 (4), 376–386.

Englert, N., 2004. Fine particles and human health–a review of epidemiological studies. Toxicol. Lett. 149 (1-3), 235–242.

Brunekreef, B., Holgate, S.T., 2002. Air pollution and health. Lancet 360 (9341), 1233–1242.

Kreyling, W.G., Semmler-Behnke, M., Möller, W., 2006. Ultrafine particle-lung interactions: does size matter? J. Aerosol. Med. 19 (1), 74–83.

Sica, A., Mantovani, A., 2012. Macrophage plasticity and polarization: in vivo veritas. J. Clin. Invest. 122 (3), 787–795.

Granata, F., Frattini, A., Loffredo, S., Staiano, R.I., Petraroli, A., Ribatti, D., Oslund, R., Gelb, M.H., Lambeau, G., Marone, G., Triggiani, M., 2010. Production of vascular endothelial growth factors from human lung macrophages induced by group IIA and group X secreted phospholipases A2. J. Immunol. 184 (9), 5232–5241.

Ferrara, A.L., Galdiero, M.R., Fiorelli, A., Cristinziano, L., Granata, F., Marone, G., Crescenzo, R.M.D., Braile, M., Marcella, S., Modestino, L., Varricchi, G., Spadaro, G., Santini, M., Loffredo, S., 2021. Macrophage-polarizing stimuli differentially modulate the inflammatory profile induced by the secreted phospholipase A2 group IA in human lung macrophages. Cytokine 138, 155378.

Bonavita, E., Galdiero, M.R., Jaillon, S., Mantovani, A., 2015. Phagocytes as Corrupted Policemen in Cancer-Related Inflammation. Adv. Cancer. Res. 128, 141–171.

Mantovani, A., Biswas, S.K., Galdiero, M.R., Sica, A., Locati, M., 2013. Macrophage plasticity and polarization in tissue repair and remodelling. J. Pathol. 229, 176–185.

Mantecca, P., Farina, F., Moschini, E., Gallinotti, D., Gualtieri, M., Rohr, A., Sancini, G., Palestini, P., Camatini, M., 2010. Comparative acute lung inflammation induced by atmospheric PM and size-fractionated tire particles. Toxicol. Lett. 198 (2), 244–254.

Farina, F., Sancini, G., Mantecca, P., Gallinotti, D., Camatini, M., Palestini, P., 2011. The acute toxic effects of particulate matter in mouse lung are related to size and season of collection. Toxicol. Lett. 202 (3), 209–217.

Longhin, E., Gualtieri, M., Capasso, L., Bengalli, R., Mollerup, S., Holme, J.A., Øvrevik, J., Casadei, S., Di Benedetto, C., Parenti, P., Camatini, M., 2016. Physico-chemical properties and biological effects of diesel and biomass particles. Environ. Pollut. 215, 366–375.

Russo, C., Apicella, B., Tregrossi, A., Oliano, M.M., Ciajolo, A., 2020. Thermophoretic sampling of large PAH (C ≥ 22–24) formed in flames. Fuel 263, 116722.

Apicella, B., Barbella, R., Ciajolo, A., Tregrossi, A., 2002. Formation of low- and high-molecular-weight hydrocarbon species in sooting ethylene flames. Combust. Sci. Technol. 174 (11-12), 309–324.

Apicella B., Russo C., Carpentieri A., Tregrossia A, Ciajoloa A. 2022. PAHs and fullerenes as structural and compositional motifs tracing and distinguishing organic carbon from soot, Fuel, 309.

Russo, C., Apicella, B., Lighty, J.S., Ciajolo, A., Tregrossi, A., 2017. Optical properties of organic carbon and soot produced in an inverse diffusion flame. Carbon 124, 372–379.

Balestrieri, B., Granata, F., Loffredo, S., Petraroli, A., Scalia, G., Morabito, P., Cardamone, C., Varricchi, G., Triggiani, M., 2021. Phenotypic and functional heterogeneity of low-density and high-density human lung macrophages. Biomedicines 9 (5), 505.

Braile, M., Fiorelli, A., Sorriento, D., Di Crescenzo, R.M., Galdiero, M.R., Marone, G., Santini, M., Varricchi, G., Loffredo, S., 2021. Human lung-resident macrophages express and are targets of thymic stromal lymphopoietin in the tumor microenvironment. Cells 10 (8), 2012.

Scorziello, A., Pellegrini, C., Secondo, A., Sirabella, R., Formisano, L., Sibaud, L., Amoroso, S., Canzoniero, L.M.T., Annunziato, L., Di Renzo, G.F., 2004. Neuronal NOS activation during oxygen and glucose deprivation triggers cerebellar granule cell death in the later reoxygenation phase. J. Neurosci. Res. 76 (6), 812–821.

Staiano, R.I., Granata, F., Secondo, A., Petraroli, A., Loffredo, S., Annunziato, L., et al., 2013. Human macrophages and monocytes express functional Na(+)/Ca (2+) exchangers 1 and 3. Adv. Exp. Med. Biol. 961, 317–326.

Grynkiewicz, G., Poenie, M., Tsien, R.Y., 1985. A new generation of Ca2+ indicators with greatly improved fluorescence properties. J. Biol. Chem. 260 (6), 3440–3450.

Triggiani, M., Granata, F., Petraroli, A., Loffredo, S., Frattini, A., Staiano, R.I., et al., 2009. Inhibition of secretory phospholipase A2-induced cytokine production in human lung macrophages by budesonide. Int. Arch. Allergy. Immunol. 150, 144–155.

Bas, S., Neff, L., Vuillet, M., Spenato, U., Seya, T., Matsumoto, M., Gabay, C., 2008. The proinflammatory cytokine response to Chlamydia trachomatis elementary bodies in human macrophages is partly mediated by a lipoprotein, the macrophage infectivity potentiator, through TLR2/TLR1/TLR6 and CD14. J. Immunol. 180 (2), 1158–1168.

Canton, M., Sanchez-Rodriguez, R., Spera, I., Venegas, F.C., Favia, M., Viola, A., et al., 2021. Reactive oxygen species in macrophages: sources and targets. Front. Immunol. 12, 734229.

Staiano, R.I., Loffredo, S., Borriello, F., Iannotti, F.A., Piscitelli, F., Orlando, P., Secondo, A., Granata, F., Lepore, M.T., Fiorelli, A., Varricchi, G., Santini, M., Triggiani, M., Di Marzo, V., Marone, G., 2016. Human lung-resident macrophages express CB1 and CB2 receptors whose activation inhibits the release of angiogenic and lymphangiogenic factors. J. Leukoc. Biol. 99 (4), 531–540.

Doster, R.S., Rogers, L.M., Gaddy, J.A., Aronoff, D.M., 2018. Macrophage extracellular traps: a scoping review. J. Innate. Immun. 10, 3–13.

Geiser, M., Kreyling, W.G., 2010. Deposition and biokinetics of inhaled nanoparticles. Part. Fibre. Toxicol. 7 (1), 2.

Oberdörster, G., Oberdörster, E., Oberdörster, J., 2005. Nanotoxicology: an emerging discipline evolving from studies of ultrafine particles. Environ. Health. Perspect. 113 (7), 823–839.

Tseng, C.-T., Perrone, L.A., Zhu, H., Makino, S., Peters, C.J., 2005. Severe acute respiratory syndrome and the innate immune responses: modulation of effector cell function without productive infection. J. Immunol. 174 (12), 7977–7985.
Arango Duque, G., Descoteaux, A., 2014. Macrophage cytokines: involvement in immunity and infectious diseases. Front. Immunol. 5, 491.
Geng, H., Meng, Z., Zhang, Q., 2006. In vitro responses of rat alveolar macrophages to particle suspensions and water-soluble components of dust storm PM(2.5). Toxicol. In Vitro 20 (5), 575–584.
Rowlands, D.J., Islam, M.N., Das, S.R., Huertas, A., Quadri, S.K., Horiuchi, K., Inamdar, N., Emin, M.T., Lindert, J., Ten, V.S., Bhattacharya, S., Bhattacharya, J., 2011. Activation of TNFR1 ectodomain shedding by mitochondrial Ca2+ determines the severity of inflammation in mouse lung microvessels. J. Clin. Invest. 121 (5), 1986–1999.
Zhao, Q., Chen, H., Yang, T., Rui, W., Liu, F., Zhang, F., Zhao, Y., Ding, W., 2016. Direct effects of airborne PM2.5 exposure on macrophage polarizations. Biochim. Biophys. Acta 1860 (12), 2835–2843.
Moller, W., Brown, D.M., Kreyling, W.G., Stone, V., 2005. Ultrafine particles cause cytoskeletal dysfunctions in macrophages: role of intracellular calcium. Part. Fibre. Toxicol. 2, 7.
Zhao, Y., Zou, W., Du, J., Zhao, Y., 2018. The origins and homeostasis of monocytes and tissue-resident macrophages in physiological situation. J. Cell. Physiol. 233 (10), 6425–6439.
Mühlfeld, C., Rothen-Rutishauser, B., Blank, F., Vanhecke, D., Ochs, M., Gehr, P., 2008. Interactions of nanoparticles with pulmonary structures and cellular responses. Am. J. Physiol. Lung. Cell. Mol. Physiol. 294 (5), L817–L829.
Weuve, J., Puett, R.C., Schwartz, J., Yanosky, J.D., Laden, F., Grodstein, F., 2012. Exposure to particulate air pollution and cognitive decline in older women. Arch. Intern. Med. 172, 219–227.
Apicella, B., Mancaruso, E., Russo, C., Tregrossi, A., Oliano, M.M., Ciajolo, A., Vaglieco, B.M., 2020. Effect of after-treatment systems on particulate matter emissions in diesel engine exhaust. Exp. Therm. Fluid. Sci. 116, 110107.
Zanobetti, A., Baccarelli, A., Schwartz, J., 2011. Gene-air pollution interaction and cardiovascular disease: a review. Prog. Cardiovasc. Dis. 53 (5), 344–352.
Woodby, B., Arnold, M.M., Valacchi, G., 2021. SARS-CoV-2 infection, COVID-19 pathogenesis, and exposure to air pollution: What is the connection? Ann. NY Acad. Sci. 1486 (1), 15–38.
Copat, C., Cristaldi, A., Fiore, M., Grasso, A., Zuccarello, P., Signorelli, S.S., Conti, G.O., Ferrante, M., 2020. The role of air pollution (PM and NO2) in COVID-19 spread and lethality: a systematic review. Environ. Res. 191, 110129.
Wang, W., Ye, L., Li, B., Gao, B., Zeng, Y., Kong, L., et al., 2007. Up-regulation of IL-6 and TNF-alpha induced by SARS-coronavirus spike protein in murine macrophages via NF-kappaB pathway. Virus. Res. 128, 1–8.
Del Valle, D.M., Kim-Schulze, S., Huang, H.-H., Beckmann, N.D., Nirenberg, S., Wang, B. o., Lavin, Y., Swartz, T.H., Madduri, D., Stock, A., Marron, T.U., Xie, H., Patel, M., Tuballes, K., Van Oekelen, O., Rahman, A., Kovatch, P., Aberg, J.A., Schadt, E., Jagannath, S., Mazumdar, M., Charney, A.W., Firpo-Betancourt, A., Mendu, D.R., Jhang, J., Reich, D., Sigel, K., Cordon-Cardo, C., Feldmann, M., Parekh, S., Merad, M., Gnjatic, S., 2020. An inflammatory cytokine signature predicts COVID-19 severity and survival. Nat. Med. 26 (10), 1636–1643.